Diffusion-weighted imaging as a treatment response biomarker evaluating bone metastases in prostate cancer: a pilot study.

Journal:	*Radiology*
Manuscript ID	RAD-16-0646.R1
Manuscript Type:	Original Research
Manuscript Categorization Terms:	MR-Diffusion Weighted Imaging < 2. MODALITIES/TECHNIQUES, Skeletal-Axial < 4. AREAS/SYSTEMS, Bone Marrow < 5. STRUCTURES, Tumor Response < 6. TOPICS, Whole Body Imaging < 6. TOPICS, Experimental Investigations < 7. METHODOLOGY

SCHOLARONE™
Manuscripts

Manuscript title

Diffusion-weighted imaging as a treatment response biomarker evaluating bone metastases in prostate cancer.

Manuscript type: Original Research

Authors

Raquel Perez-Lopez (MD, MSc), Joaquin Mateo (MD, MSc), Helen Mossop (MMathStat), Matthew D. Blackledge (PhD), David J. Collins (BMIP), Mihaela Rata (PhD), Veronica A. Morgan, Alison McDonald, Shahneen Sandhu (MD), David Lorente (MD), Pasquale Rescigno (MD), Zafeiris Zafeiriou (MD), Diletta Bianchini (MD), Nuria Porta (PhD), Emma Hall (PhD), Martin O. Leach (PhD), Johann S. De Bono (MB, ChB, PhD), Dow-Mu Koh (MD, FRCR, MRCP), Nina Tunariu (MD, FRCR, MRCP)

Institution

The Institute of Cancer Research and The Royal Marsden NHS Foundation Trust

Cancer Therapeutics Division

15 Cotswold Road

Sutton, SM2 5NG (United Kingdom)

Corresponding author information

Nina Tunariu

Radiology consultant at The Royal Marsden NHS Foundation Trust

Nina.Tunariu@icr.ac.uk

Tel.: +44 (0) 20 7352 8133

Fax: +44 (0) 20 7370 5261

- The results of this study will be partially presented at the 2016 ISMRM annual meeting (Singapore, May 2016).

Funding information

- Cancer Research UK (C12540/A12829, C12540/A13230, C1491/A9895, C1491/A15955)
- Prostate Cancer UK (PG14-016-TR2)
- Stand Up to Cancer (SU2C-AACR-DT0712)
- Prostate Cancer Foundation (20131017)
- CRUK and EPSRC in association with MRC & Dept. of Health (C1060/A10334, C1060/A16464)
- ECMC funding from Cancer Research UK and the Department of Health (CRM064X)
- BRC Funding to the Royal Marsden (BRC A38)

Manuscript title

Diffusion-weighted imaging as a treatment response biomarker evaluating bone metastases in prostate cancer: a pilot study.

Manuscript type: Original Research

Advances in knowledge

1. All six patients who responded to the Poly (ADP-ribose) polymerase (PARP) inhibitor olaparib showed a decrease in total diffusion volume (tDV) (median: -41.1%; minimum [min], maximum [max]: -58.8%, -6.3%), but no decrease was observed in any of the 15 non-responders (median: +20.7%; min, max: +0.0%, +76.9%); this difference between responders and non-responders was significant (p=0.001).
2. Increases in median apparent diffusion coefficient (mADC) of the total diffusion volume (tDV) after 12-weeks of treatment associated with responses to olaparib (OR: 1.08, 95% CI 1.00, 1.15, p=0.037).
3. When analyzing up to five target bone metastases, changes in entire volume of the target bone metastases also inversely associated with response (OR: 0.89, 95% CI 0.80, 0.99, p=0.037).

Implications for patient care

1. Clinical qualification of whole body diffusion weighted imaging (WB-DWI) as response biomarker in bone metastases would improve assessment of response to treatment in mCRPC, allowing for optimization of patients care, treatment decision and drug development in this common disease.

Summary statement

Assessment of bone metastases with whole body diffusion-weighted imaging during cancer treatment is feasible, with changes in bone metastases volume and median apparent diffusion coefficient being indicators of response to treatment in metastatic castration resistant prostate cancer in our pilot study.

ABBREVIATIONS

ADC	Apparent Diffusion Coefficient
mADC	median ADC
ALP	Alkaline Phosphatase
CI	Confidence Interval
CT	Computed Tomography
CTC	Circulating Tumor Cell
CTSU	Clinical Trials and Statistical Unit
DWI	Diffusion Weighted Imaging
FOV	Field Of View
HR	Hazard Ratio
IRB	Institutional Research Board
LDH	Lactate Dehydrogenase
mCRPC	Metastatic Castration Resistant Prostate Carcinoma
max	maximum
min	minimum
MRI	Magnetic Resonance Imaging
ρ	Spearman´s correlation coefficient
ROI	Region Of Interest
SD	Standard Deviation
tDV	total tumor Diffusion Volume
PARP	poly-(ADP)ribose polymerase
PCWG	Prostate Cancer Working Group
PTTG	Prostate Targeted Therapy Group
PSA	Prostate Specific Antigen

Q1	1st quartile
Q3	3rd quartile
WB	Whole Body

ABSTRACT

Purpose

To determine the usefulness of whole body diffusion weighted imaging (WB-DWI) to assess response of bone metastases to treatment in patients with metastatic castration resistant prostate cancer (mCRPC).

Materials and methods

A phase II prospective clinical trial of the poly-(ADP)ribose polymerase (PARP) inhibitor olaparib in mCRPC included a prospective magnetic resonance imaging (MRI) sub-study; our study was approved by Institutional Research Board (IRB), written informed consent was obtained. WB-DWI was performed at baseline and after 12-weeks of olaparib using a 1.5-T MRI. Areas of DWI signal abnormality in keeping with bone metastases were delineated to derive total diffusion volume (tDV); five target lesions were also evaluated. Associations of changes in volume of bone metastases and median apparent diffusion coefficient ADC (mADC) with response to treatment were assessed using the Mann-Whitney test and logistic regression; correlation with prostate specific antigen (PSA) and circulating tumor cell (CTC) count were assessed using Spearman's correlation (*r*).

Results

Twenty-one patients were included. All six responders to olaparib showed a decrease in tDV, while no decrease was observed in all non-responders; this difference between responders and non-responders was significant (p=0.001). Increases in mADC associated with increased odds of response (Odds Ratio [OR]:1.08, 95%CI

1.00-1.15, p=0.04). We detected a positive association between changes in tDV and best percentage change in PSA and CTC (r=0.63, 95% CI 0.27, 0.83and r=0.77, 95% CI 0.51, 0.90). When assessing five target lesions, decreases in volume were associated with response (OR for volume increase: 0.89, 95%CI 0.80-0.99, p=0.037).

Conclusion

Our pilot study showed decreases in volume and increases in mADC of bone metastases assessed by WB-DWI can potentially be used as indicators of response to olaparib in mCRPC.

INTRODUCTION

Prostate cancer is the second most commonly diagnosed cancer among men worldwide (1). Bone metastases are highly prevalent in patients with metastatic castration resistant prostate cancer (mCRPC), the late stage of prostate cancer, causing substantial disease-related morbidity and mortality in this population. Bone metastases occur in up to 84% of patients with mCRPC and frequently represent the only site of metastatic disease (2).

Standard imaging techniques, i.e. computed tomography (CT), and technetium-99m bone scintigraphy, fail to accurately evaluate the burden of bone metastases and detect changes in response to treatment (3). In fact, the widely used Response Evaluation Criteria In Solid Tumors (RECIST) 1.1 (4), do not define response in bone metastases, considering these as non-measurable disease. The Prostate Cancer Working Group 2 criteria (PCWG2) define progression in bone metastases based on the appearance of new lesions on bone scintigraphy, but fail to state any criteria for response in bone metastases (5). Therefore, tumor responses in patients with bone only metastatic disease rely solely on prostate specific antigen (PSA) falls; the latter have not been proven to be a surrogate for improved survival (5-7). There is an urgent unmet need to identify, develop, and validate non-invasive response biomarkers for bone metastases in prostate cancer.

Diffusion weighted imaging (DWI) is a functional magnetic resonance imaging (MRI) technique that studies the motion of water molecules within a tissue. Apparent diffusion coefficient (ADC) is an objective measurement of this water diffusion, which has been demonstrated to inversely correlate with cellularity in different tumor

types including bone marrow malignancies (8-13). Changes in ADC values after treatment have been correlated with tumor responses in different tumor types including myeloma, ovarian carcinoma, primary peritoneal carcinoma and rhabdomyosarcoma (14-16). Additionally, the volume of bone metastases assessed with whole body (WB) DWI has prognostic value in patients with mCRPC (17). Limited data about the value of DWI in the assessment of response to bone metastases in mCRPC is currently available, coming from small series of patients (18-21). In the setting of a prospective clinical trial, we aim to determine the usefulness of whole body diffusion weighted imaging (WB-DWI) to assess response of bone metastases to treatment in patients with metastatic castration resistant prostate cancer (mCRPC).

MATERIAL AND METHODS

We conducted a phase II trial of the poly-(ADP)ribose polymerase (PARP) inhibitor olaparib (Lynparza, AstraZeneca) in mCRPC (TOPARP-A; CRUK/11/029); patients were enrolled from July 2012 to September 2014. A prospective MRI sub-study was conducted under institutional research board (IRB) approval at The Royal Marsden NHS Foundation Trust. Enrolment to this MRI sub-study was optional; written informed consent was obtained for MRI scan acquisition.

Study design

The primary endpoint of the TOPARP-A trial was response rate, with response defined as any of the following: a response of soft tissue/visceral disease according to Response Evaluation Criteria In Solid Tumors (RECIST) 1.1(4); a confirmed reduction in the prostate specific antigen (PSA) level of ≥50%; or a conversion in the circulating tumor cell (CTC) count, with a reduction in the number of CTC from

≥5/7.5 ml of blood at baseline to <5/7.5 ml of blood during treatment, with a confirmatory assessment at least 4 weeks later (22). Detailed information of the inclusion and exclusion criteria and the results of the TOPARP-A trial have been published showing a response rate to olaparib in mCRPC of 33% (95% confidence interval [CI], 20 to 48%) (23).

Participation in the optional MRI sub-study was offered to those patients without contraindication for MRI at The Royal Marsden NHS Foundation Trust. WB-MRI was performed at baseline (within 28-days prior to starting treatment) and at Cycle 4 Day 1 (corresponding to 12-weeks after starting treatment) and every 12-weeks subsequently. The primary endpoint of the MRI sub-study was to assess the association between changes in parameters derived from WB-DWI (volume of bone metastases and median ADC) and response to olaparib. For MRI sub-study purposes, patients were classified as responders if they met the definition of the primary endpoint of the TOPARP-A trial and if they had not experienced radiological progression by 12-weeks.

Patient population in the MRI sub-study

Patients were included in this study if: a) signed informed consent for the MRI sub-study in the setting of the TOPARP-A trial, b) bone metastases identified based on review of combined imaging modalities: MRI, CT and BS (in all the cases), c) a minimum of two paired WB-MRI studies performed at baseline and after 12-weeks of treatment. Patients with suboptimal quality WB-MRI or incomplete studies were considered un-evaluable for analysis and excluded from the study.

Clinical data collection

Data were collated into an anonymized database and analyzed by the Institute of Cancer Research Clinical Trials and Statistical Unit (ICR-CTSU; London, UK). PSA and CTC counts were collected at baseline and every 12-weeks while on treatment. CTC counts were also pursued at weeks 1, 2, 4 and 8. RECIST assessments were evaluated at baseline and every 12-weeks using CT.

Whole-body MRI parameters

WB-MRI was performed on a 1.5-T MRI scanner (Avanto Siemens Healthcare, Erlangen, Germany), using surface and body coils on patients positioned supine. Axial images were acquired using free breathing single-shot twice-refocused echo-planar DWI from the upper cervical spine to mid-thighs, sequentially across four imaging stations, each consisting of 50 slices respectively. In addition to WB-DWI, anatomical imaging was also acquired using breath-hold axial T1-weighted. The scan parameters are summarized in **Appendix Table 1.**

Imaging analysis

Images were processed and analyzed with open-access imaging assistant software (OsiriX v5.6). Evaluation of T1-weighted and DWI (b50, b900 and ADC maps) was performed in order to assess the presence of metastatic bone disease. Regions of interest (ROIs) including areas of signal abnormality on DWI b900, corresponding to high signal on DWI b900 and low signal on T1-weighted imaging, in keeping with metastatic bone disease were delineated. Different delineation techniques of the signal abnormality on DWI b900 corresponding to bone metastases were undertaken. Firstly, ROI analyses were performed including all areas of signal abnormality on DWI b900

and T1-weighted MRI corresponding to bone metastases observed in the axial skeleton (spine and pelvis, not including ribs) between C4 and mid-thighs, labeled as total diffusion volume (tDV). Secondly, a more limited analysis was performed using a RECIST approach of a maximum 5 target representative bone metastases chosen using the following criteria: maximum axial dimension >1cm, well-defined lesion border and representing different skeletal areas. For this analysis, ROIs including total volume of up to 5 target lesions and ROIs including the central slice of the same target lesions were chosen.

Additionally, a single radiologist (RPL) manually delineated the entire axial skeleton (spine and pelvis, not including ribs) enclosing normal and abnormal bone marrow from C4 to lesser trochanters. This delineation technique was included in view of its possible advantage for automated segmentation of the skeleton.

A semi-automated segmentation tool from the OsiriX software v.5.6 was used for delineating ROIs. All the delineation techniques in every WB-DWI were performed by a single radiologist (RPL) with 3 years of experience in WB-DWI; manual correction of the segmentation mask corresponding to the regions of interest (ROI) was performed by the radiologist where necessary **(Figure 1)**. The volume of metastases was calculated as the number of voxels for all ROIs multiplied by the voxel volume in each case. The ADC value of every pixel was recorded and histogram representations of the ADC values of bone metastases for each patient were generated using Microsoft Excel 2010.

Statistical analysis

Distribution of PSA, CTC counts, median ADC (mADC), tDV, volume and diameter of the target lesions at baseline and percentage change after 12-weeks on treatment are presented using descriptive statistics. Baseline distributions and median changes during treatment in mADC, tDV, volume and diameter of the target lesions are compared between responders and non-responders using non-parametric Mann-Whitney tests and their association with response to treatment using univariate and multivariate (adjusting for known prognostic factors of baseline PSA, lactate dehydrogenase [LDH] and alkaline phosphatase [ALP]) logistic regression models. The correlation between baseline and changes in tDV after 12-weeks on treatment with baseline and best percentage change in PSA and CTC respectively were assessed using Spearman´s correlation coefficient (*r)*, with $0.4 \leq |r| < 0.6$ indicating moderate correlation, $0.6 \leq |r| < 0.8$ strong correlation and $|r| \geq 0.8$ very strong correlation. A significance level of 0.05 and 95% CI have been used. No adjustment for reporting of multiple analyses has been performed; therefore significant results must be interpreted with caution. The analyses are based on a data snapshot taken on 24th April 2015 and were performed with Stata version 13 (StataCorp).

RESULTS

Thirty-two of the 42 patients (76.2%; 32/42) enrolled in the TOPARP-A trial at The Royal Marsden NHS Foundation Trust consented to the MRI sub-study. Six patients did not have baseline WB-MRI due to logistic or technical issues. All 26 patients with WB-MRI at baseline had bone metastases. Of the 26 patients with baseline WB-MRI, 5 patients did not have WB-MRI at 12-weeks due to poor performance status. None of the cases were excluded due to sub-optimal quality of the WB-MRI or incomplete studies. Therefore, 21 patients had evaluable WB-MRI at baseline and after 12-weeks

of treatment **(Figure 2)**; all men, median age 68.2 years (minimum [min], maximum [max]: 40.8, 79.3 years). The population characteristics at baseline are summarized in **Table 1.** The baseline CT examinations were also reviewed using previously described terminology (24); 19 of the 21 patients had sclerotic bone metastases whereas 2 patients had mixed osteoblastic/osteolytic disease with predominantly lytic metastases. The other sites of metastatic disease outside the bone observed were in lymph nodes (57.1%; 12/21), liver (28.6%; 6/21) and lung (23.8%; 5/21). Seven patients had bone metastases only at baseline (33.3%;7/21). Six patients (29%;6/21) were considered responders to olaparib as per the primary endpoint definition and had not progressed prior to 12-weeks.

The median time between the baseline WB-MRI and starting treatment was 6-days (1^{st} quartile [Q1], 3^{rd} quartile [Q3]: 2.5, 11 days). The absolute value of the tDV, sum of the 5 target lesions total volumes and of the central slice diameters and the mADC at baseline assessed by the different delineation techniques is summarized by response status in **Table 2**. The percentage change of these parameters after 12-weeks of treatment is summarized by response status in **Table 3** and represented in box-plots in **Appendix figure 1**.

Analysis of axial skeleton DWI b900 signal abnormality

When delineating all the areas of DWI signal abnormality in keeping with bone metastases in the axial skeleton, the median tDV in this population was 0.45 L (min, max: 0.01, 1.31 L) and mADC was 782 $x10^{-6}$ mm^2/s (min, max: 684, 1121 $x10^{-6}$ mm^2/s). These parameters grouped by responders and non-responders are summarized in **Table 2**; there were no statistically significant differences between the baseline

distribution of tDV and mADC between the two groups (p=0.243 and p=0.312 respectively).

All six patients who responded to olaparib showed a decrease in tDV (median: -41.1%; min, max: -58.8%, -6.3%), but no decrease was observed in any of the 15 non-responders (median: +20.7%; min, max: +0.0%, +76.9%); this difference between responders and non-responders was significant (p=0.001). **(Table 3, Appendix figure 1)**. Patients who responded to olaparib showed a greater increase in mADC after 12-weeks of treatment (median: +35.4%; min, max: +1.3%, +59.5%), compared to non-responders (median: +7.5%; min, max: -9.0%, +32.7%, p=0.14); increases in mADC after 12-weeks of treatment were associated with increased odds of response (OR: 1.08, 95%CI 1.00, 1.15, p=0.037) **(Table 4, Appendix figure 2)**. An example of a responding patient is represented in **Figure 3**.

The two patients with mixed osteoblastic/osteolytic pattern with predominantly lytic bone metastases were non-responders who had +55.5 % and +24.6 % increase of tDV and +3.40 %, + 15.6 % increase of mADC after 12 weeks on treatment respectively.

The correlation between PSA levels, CTC counts and DWI parameters was also explored; baseline PSA levels and CTC counts showed strong and moderate positive association with baseline tDV (r=0.64, 95% CI 0.29-0.84; and r=0.59, 95% CI 0.22-0.82 respectively) and there was a strong positive association between changes in tDV and best post-treatment percentage change in PSA and CTC (r=0.63, 95% CI 0.27-0.83; and r=0.77 95% CI 0.51, 0.90 respectively), indicating that changes in tDV correlate with response to therapy.

Of the six responding patients, four had a further evaluable WB-MRI at the time of radiological and/or PSA progression. In all four cases, we observed a decrease in tDV while responding to olaparib, followed by a later increase in tDV at the time of radiological and/or PSA progression. Three of these four responding patients also had an increase in mADC while responding to treatment, followed by a decrease in mADC at the time of radiological and/or PSA progression. The fourth patient experienced minimal mADC change at PSA nadir and disease progression. **(Appendix figures 3 and 4)**.

Analysis of five target lesions (total volume and central slice)

With the aim of evaluating more limited radiological analyses, to decrease workload, we correlated changes in up to 5 target lesions per patient with treatment response. We evaluated 5 target lesions in 19 of the 21 patients (90%); the remaining two patients had only one and three evaluable bone lesions respectively. The median sum of total volumes corresponding to the target lesions in the population at baseline was 0.05 L (min, max: 0.01, 0.52 L), and the mADC when delineating total volume of the target lesions was 814 $x10^{-6}$ mm^2/s (min, max: 606, 1712$x10^{-6}$ mm^2/s). In patients with non-widespread bone disease (N=9) we also assessed the diameter of the target lesions in the central slice. When assessing only the central slice of the same target lesions, the median of the sum of diameters at baseline was 12.6mm (min, max: 2.8, 20.2 mm) and the mADC was 835 $x10^{-6}$ mm^2/s (min, max: 554.5, 1263 $x10^{-6}$ mm/s). These parameters grouped by responders and non-responders are summarized in **Table 2**; there were no statistically significant differences between the baseline distribution of volume, diameter and mADC (central slice and volume) of the target

lesions between the two groups (p=0.876, p=0.143, p=0.312 and, p=0.073 respectively).

Then, we assessed the same target lesions for each patient in their follow-up WB-MRI after 12-weeks of treatment; the percentage change of these parameters after 12-weeks of treatment is summarized by response status in **Table 3, Figure 2**. Changes in entire lesion volume of the target bone metastases also inversely associated with response (OR: 0.89, 95%CI 0.80, 0.99, p=0.037) **(Table 4).** The mADC change at 12-weeks, when analyzing the target bone metastases (total volume and central slice), also associated with response, although these associations did not reach statistical significance (p=0.056 and p=0.082 respectively) **(Table 4)**. Results from the multivariate logistic regression analyses showed similar trends (**Table 4**).

Analysis of the axial skeleton (enclosing normal and abnormal bone marrow)

The baseline median of the mADC in our population when delineating the entire axial skeleton including both normal and abnormal bone marrow was 805 $x10^{-6}$ mm^2/s (min, max: 614, 1182 $x10^{-6}$ mm^2/s). mADC at baseline grouped by responders and non-responders are summarized in **Table 2**; there were no statistically significant differences between the baseline distributions of mADC between the two groups (p=0.94). The percentage change of mADC after 12-weeks of treatment is summarized by response status in **Table 3**, **Figure 2**. When comparing the mADC of the entire axial skeleton (normal and abnormal bone marrow) pre- and-post treatment with olaparib, changes in mADC did not associate with response to treatment (p=0.518). **(Table 4)**

DISCUSSION

We hypothesized that changes in volume of bone marrow metastases assessed by DWI and changes in mADC are indicators of response of bone metastases to treatment in patients with mCRPC. In our study we explored different delineation techniques for assessing bone metastases quantitatively and qualitatively with WB-DWI. One technique included all the areas of DWI signal abnormality in keeping with all bone metastases in the axial skeleton (tDV); the other focused on two simpler techniques assessing five target lesions, based on the widely used RECIST 1.1 (4), to determine whether a simplified approach may be viable in clinical practice. Finally, we explored if changes in mADC delineating the entire spine and pelvis (including areas of normal and abnormal bone marrow), which may facilitate automated delineation, was associated to response.

We have shown that when delineating all the areas of DWI signal abnormality in keeping with bone metastases in the axial skeleton (from C4 to mid-thigh), the changes detected in tDV and mADC after 12-weeks on treatment allow the identification of responders in mCRPC with bone metastases. Decreases in tDV correlated with decreases in PSA levels and CTC count falls, and also with overall response as defined as a composite endpoint in the TOPARP-A clinical trial (23). Consistent with the fact that tumor cell death results in increased water diffusivity manifested as higher ADC values, patients who responded to olaparib also showed a greater increase in mADC compared to non-responders. In our population, the results of simpler ways of assessing bone metastases on WB-DWI in 5 selected target lesions (total volume or central slice) support further evaluation of this faster and more practical approach in future studies; as decreases in volume and diameter of the five

target lesions after 12-weeks on treatment associated with response. There was also a trend of significance when associating mADC increases of the target lesions at 12-weeks and response. Therefore, overall, these data indicate that WB-DWI may have a role in bone metastases response assessment in mCRPC, without need of ionizing radiation or intravenous contrast, potentially allowing the detection of differential responses in visceral or nodal metastases and bone metastases. Clinical qualification of WB-DWI as response biomarker in bone metastases would improve assessment of response to treatment in mCRPC, allowing for optimization of patients care, treatment decision and drug development in this common disease. Conversely, when delineating spine and pelvis, including all areas of normal and abnormal bone marrow, increases in mADC after 12-weeks on treatment did not associate to response; probably due to the fact that changes in mADC in bone metastases are diluted by the absence of changes in mADC in normal bone marrow.

We acknowledge the potential limitations of our study; firstly, due to the small size of this pilot study, only limited exploration of the impact of adjustment for other clinical factors on the association of changes in tDV and mADC is possible. Analyzing larger populations in multi-center studies is now needed for future validation of these results and to allow multivariate analyses. Secondly, all our patients were treated with one drug, the PARP inhibitor olaparib; however, previous studies have identified similar changes in DWI in bone metastases responding to hormonal therapy and cytotoxics (18-21). Prospective studies to replicate our results with established treatments for mCRPC are now needed. Thirdly, it should be noted that the ROI delineation depends on the quality of the acquired DWI data, the semi-automatic segmentation tool and radiologist expertise. Prior studies reported high intra-reader reproducibility of DWI

analysis using similar bone metastases delineation methodology (17, 25), although this needs to be validated in larger, properly powered studies. Finally, we acknowledge that the majority of our population had sclerotic bone metastases, only 2 patients had predominantly lytic bone metastases; therefore, it was not feasible to perform comparison between the sclerotic vs lytic nature of the bone metastases. Despite these limitations, our study represents the largest prospective series to date in a trial of a novel therapeutic assessing response to drug treatment in bone metastases in patients with mCRPC using WB-DWI. The data presented here highlight the potential of DWI for bone metastases response assessment and warrants further evaluation of WB-DWI in this disease.

In conclusion, we have shown that assessment of bone metastases with WB-DWI during anticancer treatment is feasible, with changes in bone metastases volume and mADC being indicators of response to treatment in mCRPC in our pilot study. Moreover, the more efficient study of five target lesions has substantial practical merit for disease evaluation, which can be more easily adopted into clinical practice. These results support further evaluation of DWI as a response biomarker in prospective mCRPC patient cohorts, ideally embedded into clinical trials (26).

ACKNOWLEDGEMENTS

Supported by grants from Cancer Research UK (C12540/ A12829, C12540/A13230, C1491/A9895, and C1491/A15955, for trial CRUK/11/029), Stand Up To Cancer–Prostate Cancer Foundation (a Prostate Dream Team Translational Cancer Research Grant), and Prostate Cancer UK. This study was conducted with support from the Investigator-Sponsored Study Collaboration between AstraZeneca and the National Institute for Health Research Cancer Research Network, MRC-Prostate Cancer UK Fellowship to J.M. and NIHR postdoctoral fellowship to M.D.B (NHR011X). We acknowledge CRUK and EPSRC support to the Cancer Imaging Centre at ICR and RMH in association with MRC & Dept. of Health; contract grant numbers: C1060/A10334, C1060/A16464; NHS funding to the NIHR Biomedicine Research Centre and the Clinical Research Facility. This work was undertaken at The Royal Marsden NHS Foundation Trust which received a proportion of its funding from the NHS Executive; the views expressed in this publication are those of the authors and not necessarily those of the NHS Executive. M.O.L. is an NIHR Senior Investigator. Raquel Perez-Lopez conducted this work in the Medicine Doctorate framework of the Universidad Autonoma de Barcelona.

REFERENCES

1. Ferlay J, Soerjomataram I, Dikshit R, et al. Cancer incidence and mortality worldwide: sources, methods and major patterns in GLOBOCAN 2012. Int J Cancer. 2015;136(5):E359-386.
2. Gandaglia G, Abdollah F, Schiffmann J, et al. Distribution of metastatic sites in patients with prostate cancer: A population-based analysis. Prostate. 2014;74(2):210-216.
3. Jambor I, Kuisma A, Ramadan S, et al. Prospective evaluation of planar bone scintigraphy, SPECT, SPECT/CT, F-NaF PET/CT and whole body 1.5T MRI, including DWI, for the detection of bone metastases in high risk breast and prostate cancer patients: SKELETA clinical trial. Acta Oncol. 2015:1-9.
4. Eisenhauer EA, Therasse P, Bogaerts J, et al. New response evaluation criteria in solid tumours: revised RECIST guideline (version 1.1). Eur J Cancer. 2009;45(2):228-247.
5. Scher HI, Halabi S, Tannock I, et al. Design and end points of clinical trials for patients with progressive prostate cancer and castrate levels of testosterone: recommendations of the Prostate Cancer Clinical Trials Working Group. J Clin Oncol. 2008;26(7):1148-1159.
6. Berthold DR, Pond GR, Roessner M, et al. Treatment of hormone-refractory prostate cancer with docetaxel or mitoxantrone: relationships between prostate-specific antigen, pain, and quality of life response and survival in the TAX-327 study. Clin Cancer Res. 2008;14(9):2763-2767.
7. Halabi S, Armstrong AJ, Sartor O, et al. Prostate-specific antigen changes as surrogate for overall survival in men with metastatic castration-resistant prostate cancer treated with second-line chemotherapy. J Clin Oncol. 2013;31(31):3944-3950.
8. Guo AC, Cummings TJ, Dash RC,Provenzale JM. Lymphomas and high-grade astrocytomas: comparison of water diffusibility and histologic characteristics. Radiology. 2002;224(1):177-183.
9. Hayashida Y, Hirai T, Morishita S, et al. Diffusion-weighted imaging of metastatic brain tumors: comparison with histologic type and tumor cellularity. AJNR Am J Neuroradiol. 2006;27(7):1419-1425.
10. Zelhof B, Pickles M, Liney G, et al. Correlation of diffusion-weighted magnetic resonance data with cellularity in prostate cancer. BJU Int. 2009;103(7):883-888.
11. Liu Y, Ye Z, Sun H,Bai R. Clinical Application of Diffusion-Weighted Magnetic Resonance Imaging in Uterine Cervical Cancer. Int J Gynecol Cancer. 2015;25(6):1073-1078.
12. Matsubayashi RN, Fujii T, Yasumori K, Muranaka T,Momosaki S. Apparent Diffusion Coefficient in Invasive Ductal Breast Carcinoma: Correlation with Detailed Histologic Features and the Enhancement Ratio on Dynamic Contrast-Enhanced MR Images. J Oncol. 2010;2010.
13. Nonomura Y, Yasumoto M, Yoshimura R, et al. Relationship between bone marrow cellularity and apparent diffusion coefficient. J Magn Reson Imaging. 2001;13(5):757-760.
14. Thoeny HC, De Keyzer F, Chen F, et al. Diffusion-weighted MR imaging in monitoring the effect of a vascular targeting agent on rhabdomyosarcoma in rats. Radiology. 2005;234(3):756-764.

15. Kyriazi S, Collins DJ, Messiou C, et al. Metastatic ovarian and primary peritoneal cancer: assessing chemotherapy response with diffusion-weighted MR imaging--value of histogram analysis of apparent diffusion coefficients. Radiology. 2011;261(1):182-192.
16. Giles SL, Messiou C, Collins DJ, et al. Whole-body diffusion-weighted MR imaging for assessment of treatment response in myeloma. Radiology. 2014;271(3):785-794.
17. Perez-Lopez R, Lorente D, Blackledge MD, et al. Volume of Bone Metastasis Assessed with Whole-Body Diffusion-weighted Imaging Is Associated with Overall Survival in Metastatic Castration-resistant Prostate Cancer. Radiology. 2016:150799.
18. Blackledge MD, Collins DJ, Tunariu N, et al. Assessment of treatment response by total tumor volume and global apparent diffusion coefficient using diffusion-weighted MRI in patients with metastatic bone disease: a feasibility study. PLoS One. 2014;9(4):e91779.
19. Reischauer C, Froehlich JM, Koh DM, et al. Bone metastases from prostate cancer: assessing treatment response by using diffusion-weighted imaging and functional diffusion maps--initial observations. Radiology. 2010;257(2):523-531.
20. Lee KC, Bradley DA, Hussain M, et al. A feasibility study evaluating the functional diffusion map as a predictive imaging biomarker for detection of treatment response in a patient with metastatic prostate cancer to the bone. Neoplasia. 2007;9(12):1003-1011.
21. Messiou C, Collins DJ, Giles S, de Bono JS, Bianchini D,de Souza NM. Assessing response in bone metastases in prostate cancer with diffusion weighted MRI. Eur Radiol. 2011;21(10):2169-2177.
22. Olmos D, Arkenau HT, Ang JE, et al. Circulating tumour cell (CTC) counts as intermediate end points in castration-resistant prostate cancer (CRPC): a single-centre experience. Ann Oncol. 2009;20(1):27-33.
23. Mateo J, Carreira S, Sandhu S, et al. DNA-Repair Defects and Olaparib in Metastatic Prostate Cancer. N Engl J Med. 2015;373(18):1697-1708.
24. Vargas HA, Wassberg C, Fox JJ, et al. Bone metastases in castration-resistant prostate cancer: associations between morphologic CT patterns, glycolytic activity, and androgen receptor expression on PET and overall survival. Radiology. 2014;271(1):220-229.
25. Blackledge MD, Tunariu N, Orton MR, et al. Inter- and Intra-Observer Repeatability of Quantitative Whole-Body, Diffusion-Weighted Imaging (WBDWI) in Metastatic Bone Disease. PLoS One. 2016;11(4):e0153840.
26. Yap TA, Sandhu SK, Workman P,de Bono JS. Envisioning the future of early anticancer drug development. Nat Rev Cancer. 2010;10(7):514-523.

Table 1. Baseline characteristics and prior treatments of the overall population included in the whole body MRI study (N=21).

Q1: 1st quartile, Q3: 3rd quartile

Clinical characteristics	Median (Q1, Q3)	Min, max
Hemoglobin (g/dL)	10.9 (10.2, 11.5)	9.2, 14.2
Prostate Specific Antigen (ng/mL)	411 (146, 806)	19, 2949
Alkaline Phosphatase (IU/L)	147 (86, 363)	54, 2652
Lactate Dehydrogenase (IU/L)	234 (176, 318)	109, 862
Albumin (g/dL)	3.5 (3.1, 3.7)	2.7, 4.0
Circulating Tumor Cell count (number/7.5ml)	46 (8, 102)	3, 187
Prior treatments	No.	%
Docetaxel	21	100.0
Cabazitaxel	11	52.4
Abiraterone acetate	19	90.5
Enzalutamide	4	19.0
Radium-223	1	4.8
Bisphosphonates	4	19.0
Palliative radiotherapy to bone	6	28.6
Sites of metastatic disease	No.	%
Bone	21	100
Nodal	12	57.1
Liver	6	28.6
Lung	5	23.8
Bone only	7	33.3

Table 2. Baseline circulating tumor cells (CTC) count, prostate specific antigen (PSA) and characteristics of the bone metastases assessed by whole body diffusion weighted imaging (WB-DWI) with the different delineation techniques in responders and non-responder patients.

Q1: 1st quartile, Q3: 3rd quartile

	Responders			Non-responders			*Mann-Whitney p-value*
	N	Median (Q1, Q3)	Min, max	N	Median (Q1, Q3)	Min, max	
Clinical characteristics							
CTC (number/7.5ml)	6	63 (8, 102)	3, 105	15	46 (8, 104)	6, 187	0.845
PSA (ng/ml)	6	868 (34, 1847)	28, 2949	15	381 (146, 456)	19, 1505	0.350
Axial skeleton DWI signal abnormality							
Volume (L)	6	0.83 (0.17, 1.01)	0.16, 1.31	15	0.44 (0.16, 0.79)	0.01, 1.07	0.243
Median ADC ($x10^{-6}$ mm^2/s)	6	847 (775, 921)	693, 1121	15	748 (726, 915)	684, 1023	0.312
Up to 5 target lesions							
Volume (L)	6	0.05 (0.04, 0.06)	0.04, 0.09	15	0.05 (0.02, 0.12)	0.01, 0.52	0.876
Median ADC ($x10^{-6}$ mm^2/s)	6	859 (814, 900)	606, 1712	15	737 (695, 865)	624, 1017	0.312
Central slice 5 target lesions							
Diameter (mm)	2	15.3 (14.3, 16.3)	14.3, 16.3	7	11.6 (7.5, 13.1)	2.8, 20.2	0.143
Median ADC ($x10^{-6}$ mm^2/s)	6	941 (867, 1002)	555, 1263	15	743 (673, 852)	575, 1083	0.073
Entire axial skeleton							
Median ADC ($x10^{-6}$ mm^2/s)	6	808 (650, 1093)	614, 1182	15	805 (751, 1002)	722, 1039	0.938

Table 3. Percentage change after 12 weeks on treatment of the circulating tumor cells (CTC) counts, prostate specific antigen (PSA) and the parameters derived from the whole body diffusion weighted imaging (WB-DWI) analysis with the different delineation techniques in responders and non-responders patients.

% change after 12 weeks	Responders			Non-responders			*Mann-Whitney p-value*
	N	Median (Q1, Q3)	Min, max	N	Median (Q1, Q3)	Min, max	
Clinical characteristics							
CTC (number/7.5ml)	6	-96.0 (-100, -82.9)	-100, -60.5	15	-2.9 (-37.5, 75.0)	-73.8, 312.5	NA*
PSA (ng/ml)	6	-68.6 (-80.1, -37.5)	-94.6, -29.3	15	89.9 (36.0, 239.0)	-14.4, 525.6	NA*
Axial skeleton DWI signal abnormality							
Volume (L)	6	-41.1 (-52.9, -28.7)	-58.8, -6.3	15	20.7 (3.2, 53.0)	0.0, 76.9	0.001
Median ADC ($x10^{-6}$ mm^2/s)	6	35.4 (3.8, 44.1)	1.3, 59.5	15	7.5 (3.7, 15.6)	-9.0, 32.7	0.139
Up to 5 target lesions							
Volume (L)	6	-25.5 (-57.0, -18.2)	-78.7, 4.54	15	14.6 (0.0, 47.5)	-20.2, 76.9	0.002
Median ADC ($x10^{-6}$ mm^2/s)	6	26.3 (11.4, 47.4)	4.8, 102.9	15	7.4 (-2.3, 12.9)	-10.8, 25.6	0.024
Central slice 5 target lesions							
Diameter (mm)	2	-59.2 (-88.3, -30.1)	-88.3, -30.1	7	3.8 (1.6, 41.4)	0.0, 69.9	0.040
Median ADC ($x10^{-6}$ mm^2/s)	6	27.4 (14.0, 47.0)	12.8, 52.3	15	10.0 (3.2, 17.2)	-12.7, 63.1	0.018
Entire axial skeleton							
Median ADC ($x10^{-6}$ mm^2/s)	6	7.4 (-0.8, 26.0)	-16.6, 29.0	15	5.6 (3.4, 12.5)	-21.6, 16.7	0.876

* Changes in CTC and PSA were used to define response/non-response therefore formal comparisons have not been made.

Table 4. Associations of total diffusion volume (tDV), volume and diameter of the target lesions and median ADC (mADC) changes between baseline and 12 weeks with binary response to treatment were assessed using logistic regression.

OR: Odds ratio

	N	Univariate		Multivariate†	
		OR (95% CI)	**p-value**	**OR (95% CI)**	**p-value**
	Axial skeleton DWI signal abnormality				
Volume (L)	21	Not-calculable*		Not-calculable*	
Median ADC ($x10^{-6}$ mm^2/s)	21	1.08 (1.00, 1.15)	0.037	1.16 (1.01, 1.33)	0.04
	Up to 5 target lesions				
Volume (L)	21	0.89 (0.80, 0.99)	0.037	0.53 (0.09, 3.15)	0.48
Median ADC ($x10^{-6}$ mm^2/s)	21	1.10 (1.00, 1.22)	0.056	1.13 (0.95, 1.33)	0.17
	Central slice 5 target lesions				
Median ADC ($x10^{-6}$ mm^2/s)	21	1.05 (0.99, 1.11)	0.082	1.07 (0.99, 1.15)	0.07
	Entire axial skeleton				
Median ADC ($x10^{-6}$ mm^2/s)	21	1.03 (0.94, 1.12)	0.518	1.03 (0.93, 1.15)	0.56

*Unable to fit model as change in volume <0% predicts data perfectly

† Adjusting for baseline PSA, LDH and ALP

Figure 1. Images show the different delineation techniques in two-dimensional coronal or axial views for illustrative purpose. Areas of signal abnormality

corresponding to high signal intensity on DWI (b = 900 mm/s^2) and low signal intensity on T1-weighted image, in keeping with bone metastases observed between C4 and the mid-thigh were delineated on DWI (b= 900mm/s^2) (a). In order to explore a more limited approach, total volume (b) and central axial slice (c) of up to 5 target lesions were delineated on DWI (b= 900mm/s^2). (d) Finally, the entire axial skeleton including areas of normal and abnormal signal abnormality was delineated.

Figure 2. Consort diagram of study selection process.

Figure 3. Images of mCRPC in a 70-year-old man responding to olaparib showing reduction in the b900 DWI signal abnormality extent on maximum intensity projection images (b=900 s/mm^2) at baseline (a) and after 12 weeks of treatment (b). The histogram (c) depicts the ADC values of the tDV at baseline and after 12 weeks on treatment, showing an increase in the mADC.

Appendix table 1. Imaging parameters for whole body MRI.

PARAMETER	T1 weighted imaging	DWI
MRI platform	1.5-T scanner (Avanto, Siemens Healthcare)	
Type of pulse sequence	Spoiled gradient echo (FLASH)	Single-shot twice-refocused echo-planar imaging
Respiration	Breath-hold	Free-breathing
Type of acquisition	2D	2D
Field of view (mm)	380-420	380-420
Repetition time (ms)	380	14000
Echo time (ms)	5	68
Inversion time (ms)	NA	180
Flip angle	70	90
Fat suppression	NA	STIR
Receiver bandwidth (Hz/pixel)	331	1800
Number of signal average	1	4
Section thickness (mm)	5	5
b factors (s/mm^2)	NA	50 and 900
Number stations	4 (50 slices each)	4 (50 slices each)

Note: A 1.5-T MR scanner (Avanto, Siemens Healthcare) was used for imaging. DWI= Diffusion Weighted Imaging, FLASH = fast low-angle shot, NA = not applicable, STIR = short inversion time inversion recovery, 2D = two-dimensional.

Appendix figure 1. Box-plots of (a) percentage volume/diameter change of bone metastases, delineated on axial DWb900, and (b) median apparent diffusion coefficient (mADC) at 12 weeks assessed by different delineation techniques.

*** Logistic regression ($p<0.05$)**

Appendix figure 2. Scatter plot of total diffusion volume (tDV) and median apparent diffusion coefficient (mADC) change when delineating axial skeleton diffusion signal abnormality in responders (green circles) and non-responders (red crosses).

Appendix figure 3. Scatter plots of percentage change of total diffusion volume (tDV) (triangles) and median apparent diffusion coefficient (mADC) (circles) at response and disease progression in those 4 responder patients with evaluable whole body MRI.

Appendix figure 4. Images in a 70-year-old mCRPC man on olaparib. Initially, the 12 weeks axial MRI images showed a reduction of the DWI ($b = 900$ mm/s^2) signal abnormality extent in the lumbar vertebrae bone metastases and an increase in mADC values compared to baseline; subsequently a follow-up MRI showed an increase of signal abnormality extent on DWI ($b = 900$ mm/s^2) and a decrease in the mADC values in the same bone metastases, in keeping with disease progression. The histogram depicts the ADC values of the tDV at baseline, after 12 weeks on treatment and at progression.

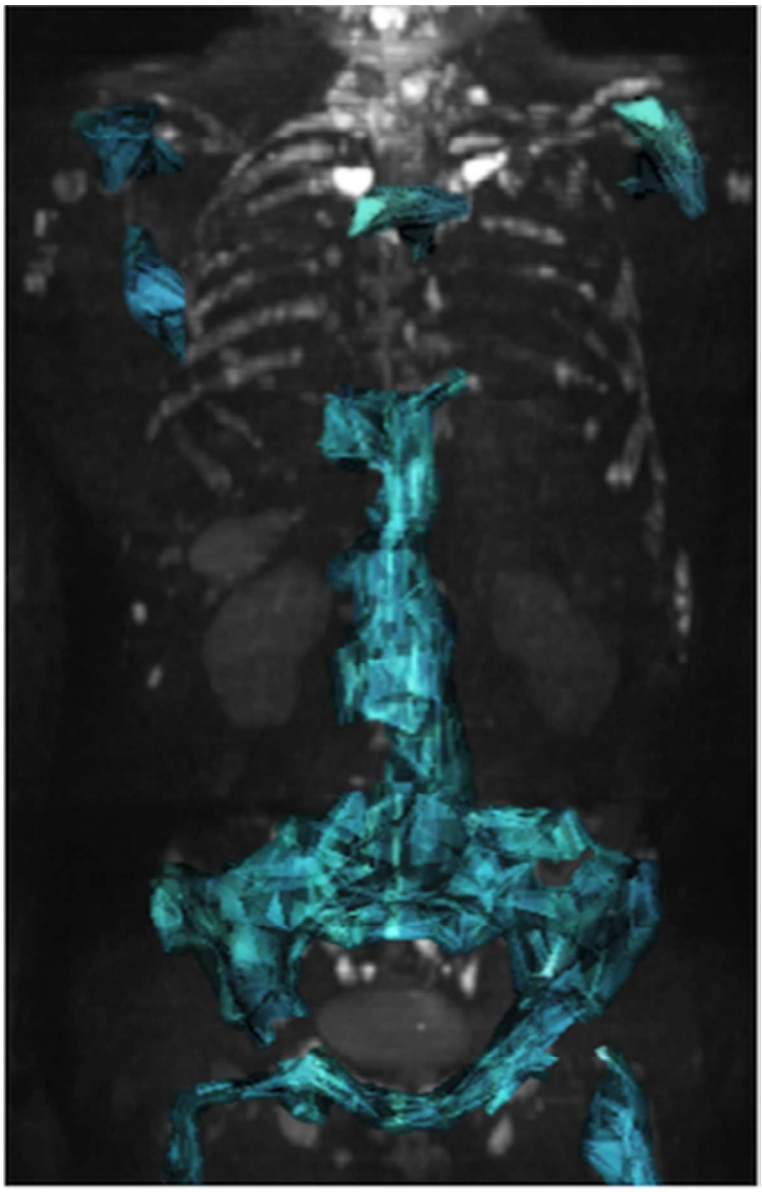

Figure 1a. Images show the different delineation techniques in two-dimensional coronal or axial views for illustrative purpose. Areas of signal abnormality corresponding to high signal intensity on DWI (b = 900 mm/s^2) and low signal intensity on T1-weighted image, in keeping with bone metastases observed between C4 and the mid-thigh were delineated on DWI (b= 900mm/s^2) (a). In order to explore a more limited approach, total volume (b) and central axial slice (c) of up to 5 target lesions were delineated on DWI (b= 900mm/s^2). (d) Finally, the entire axial skeleton including areas of normal and abnormal signal abnormality was delineated.

Figure 1
32x50mm (300 x 300 DPI)

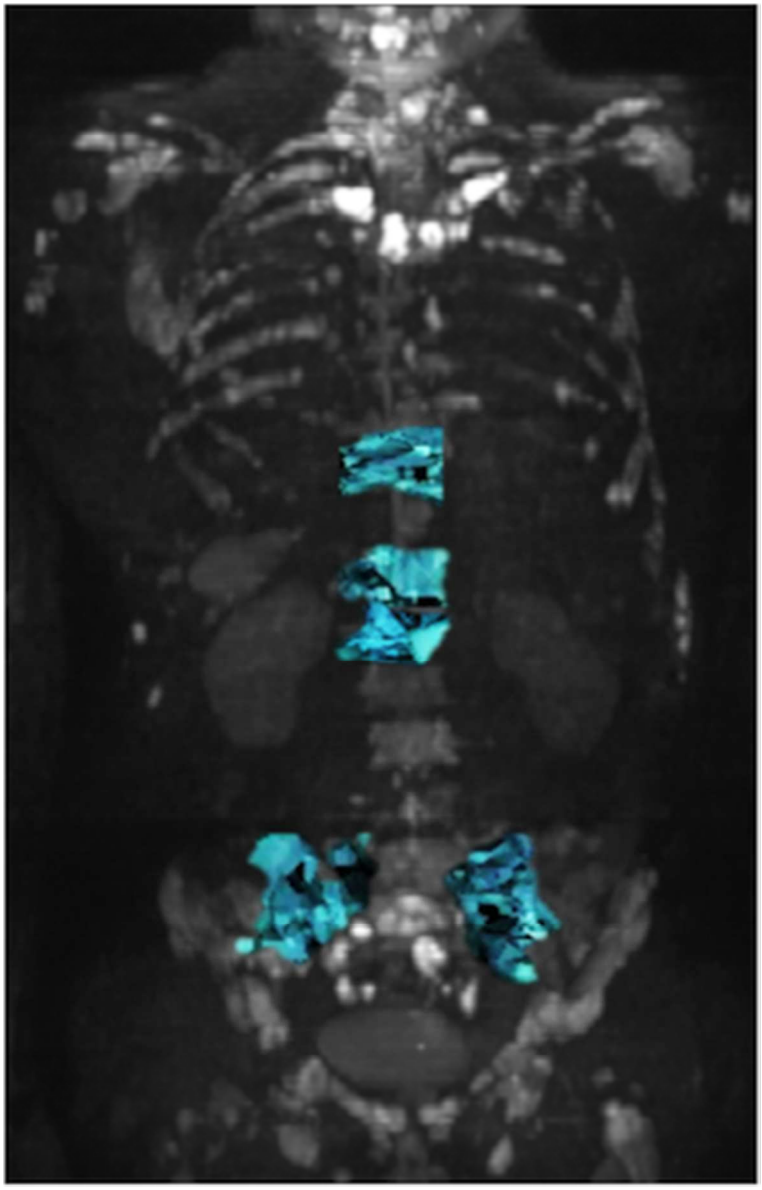

Figure 1b. Images show the different delineation techniques in two-dimensional coronal or axial views for illustrative purpose. Areas of signal abnormality corresponding to high signal intensity on DWI (b = 900 mm/s^2) and low signal intensity on T1-weighted image, in keeping with bone metastases observed between C4 and the mid-thigh were delineated on DWI (b= 900mm/s^2) (a). In order to explore a more limited approach, total volume (b) and central axial slice (c) of up to 5 target lesions were delineated on DWI (b= 900mm/s^2). (d) Finally, the entire axial skeleton including areas of normal and abnormal signal abnormality was delineated.

Figure 1
32x50mm (300 x 300 DPI)

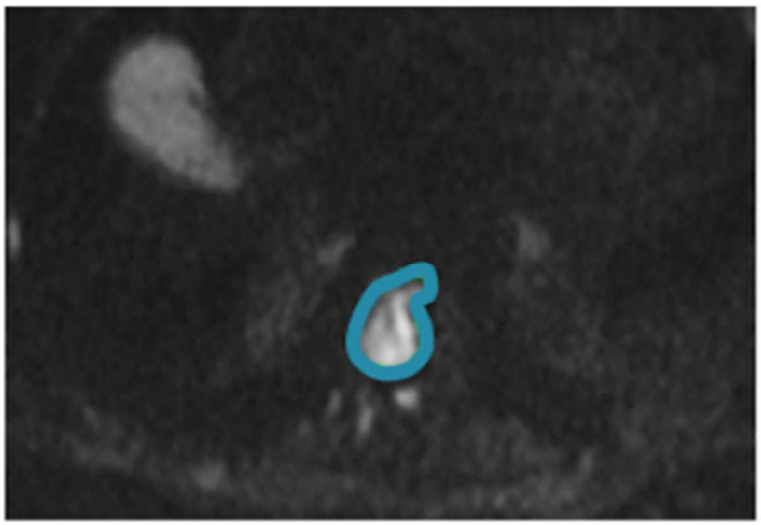

Figure 1c. Images show the different delineation techniques in two-dimensional coronal or axial views for illustrative purpose. Areas of signal abnormality corresponding to high signal intensity on DWI (b = 900 mm/s^2) and low signal intensity on T1-weighted image, in keeping with bone metastases observed between C4 and the mid-thigh were delineated on DWI (b= 900mm/s^2) (a). In order to explore a more limited approach, total volume (b) and central axial slice (c) of up to 5 target lesions were delineated on DWI (b= 900mm/s^2). (d) Finally, the entire axial skeleton including areas of normal and abnormal signal abnormality was delineated.

Figure 1
32x22mm (300 x 300 DPI)

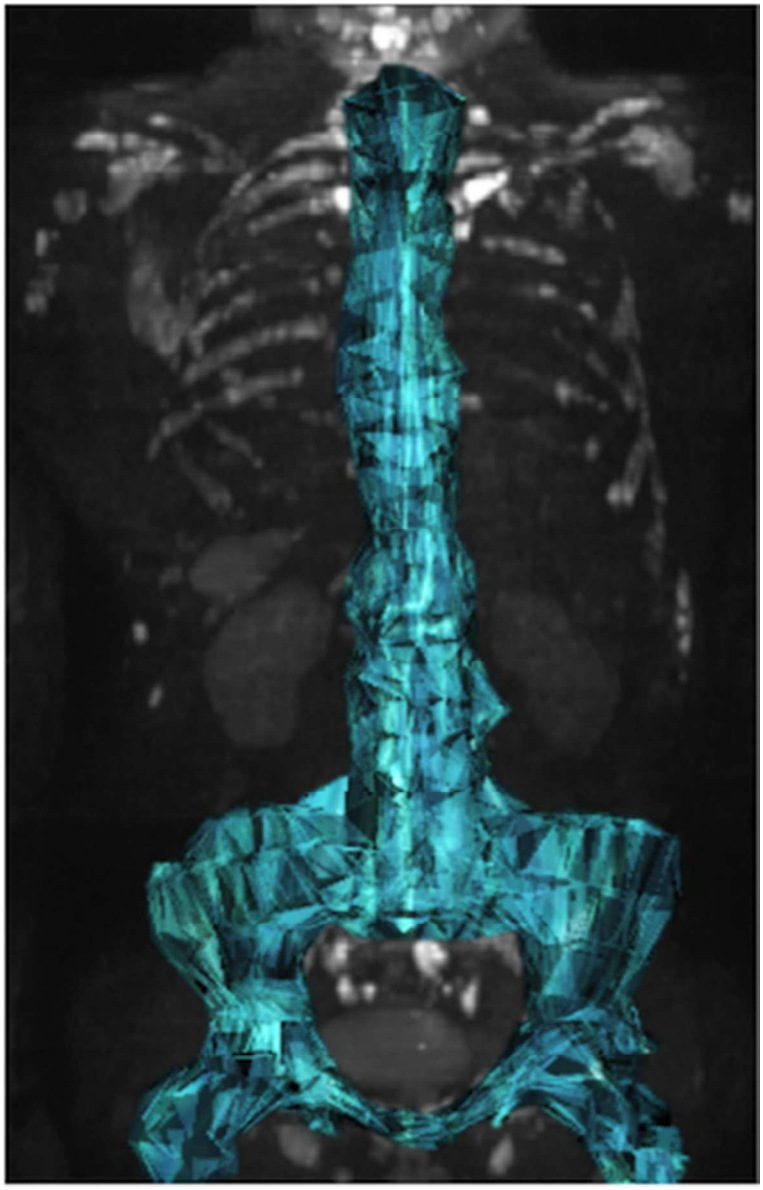

Figure 1d. Images show the different delineation techniques in two-dimensional coronal or axial views for illustrative purpose. Areas of signal abnormality corresponding to high signal intensity on DWI (b = 900 mm/s^2) and low signal intensity on T1-weighted image, in keeping with bone metastases observed between C4 and the mid-thigh were delineated on DWI (b= 900mm/s^2) (a). In order to explore a more limited approach, total volume (b) and central axial slice (c) of up to 5 target lesions were delineated on DWI (b= 900mm/s^2). (d) Finally, the entire axial skeleton including areas of normal and abnormal signal abnormality was delineated.

Figure 1
32x50mm (300 x 300 DPI)

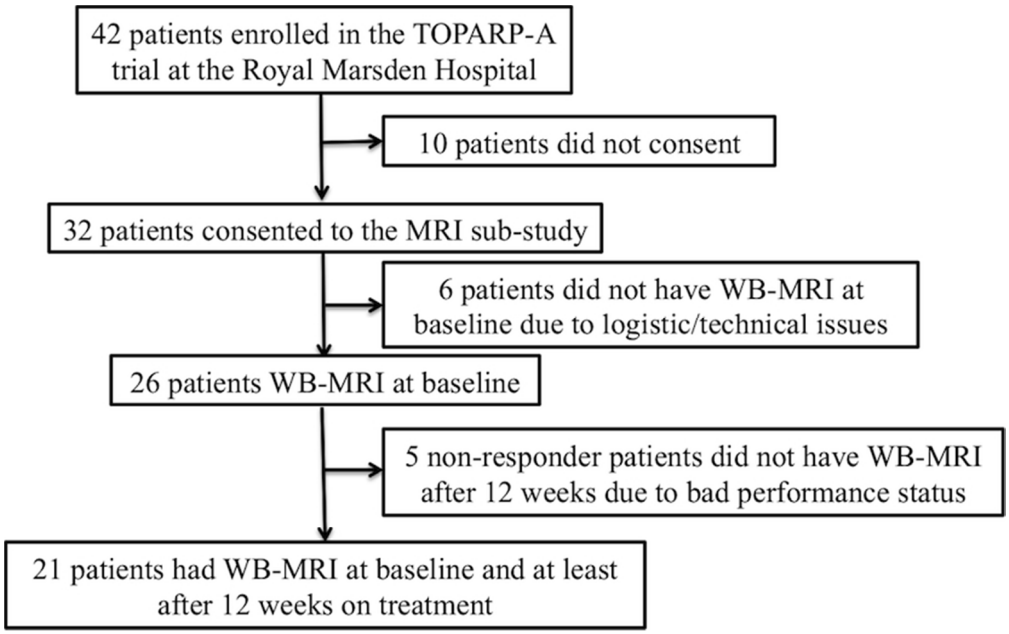

Figure 2. Consort diaphragm of study selection process.
Figure 2
70x43mm (300 x 300 DPI)

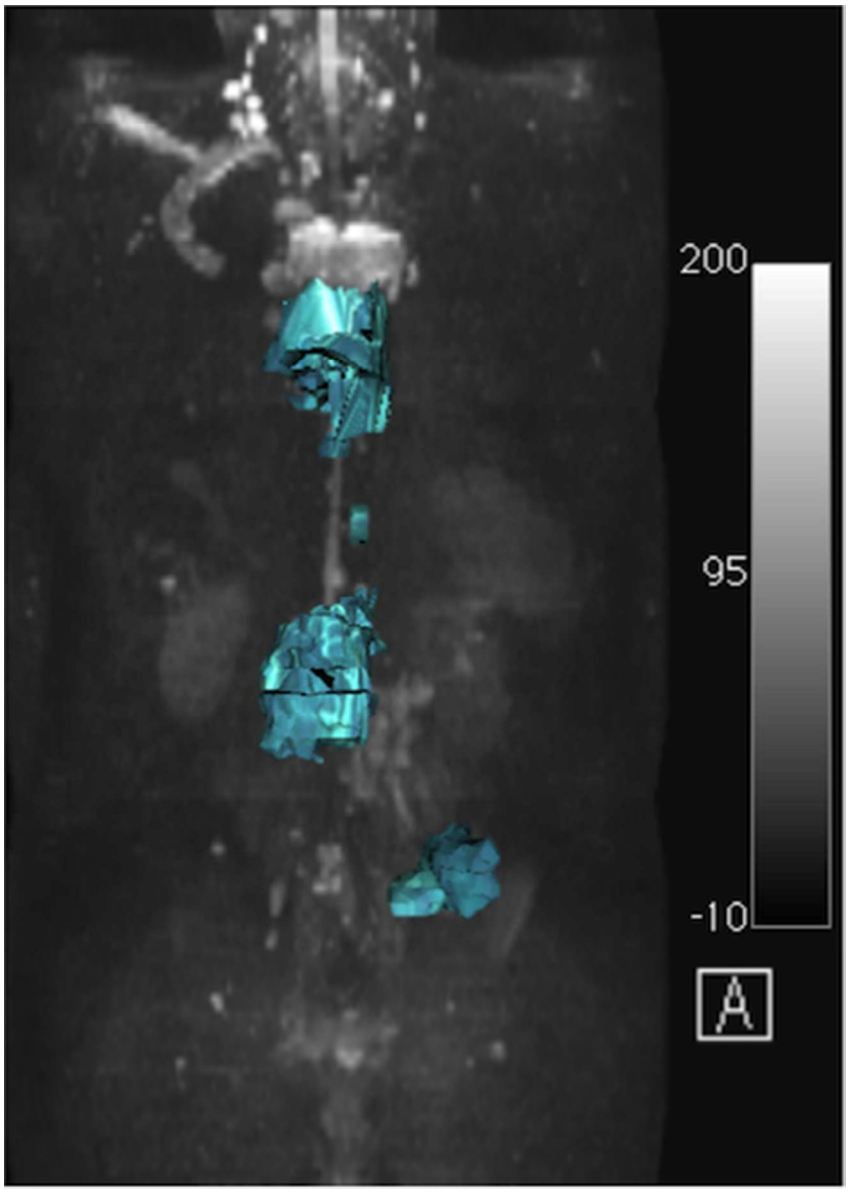

Figure 3a. Images of mCRPC in a 70-year-old man responding to olaparib showing reduction in the b900 DWI signal abnormality extent on maximum intensity projection images (b=900 s/mm^2) at baseline (a) and after 12 weeks of treatment (b). The histogram (c) depicts the ADC values of the tDV at baseline and after 12 weeks on treatment, showing an increase in the mADC.

Figure 3
35x50mm (300 x 300 DPI)

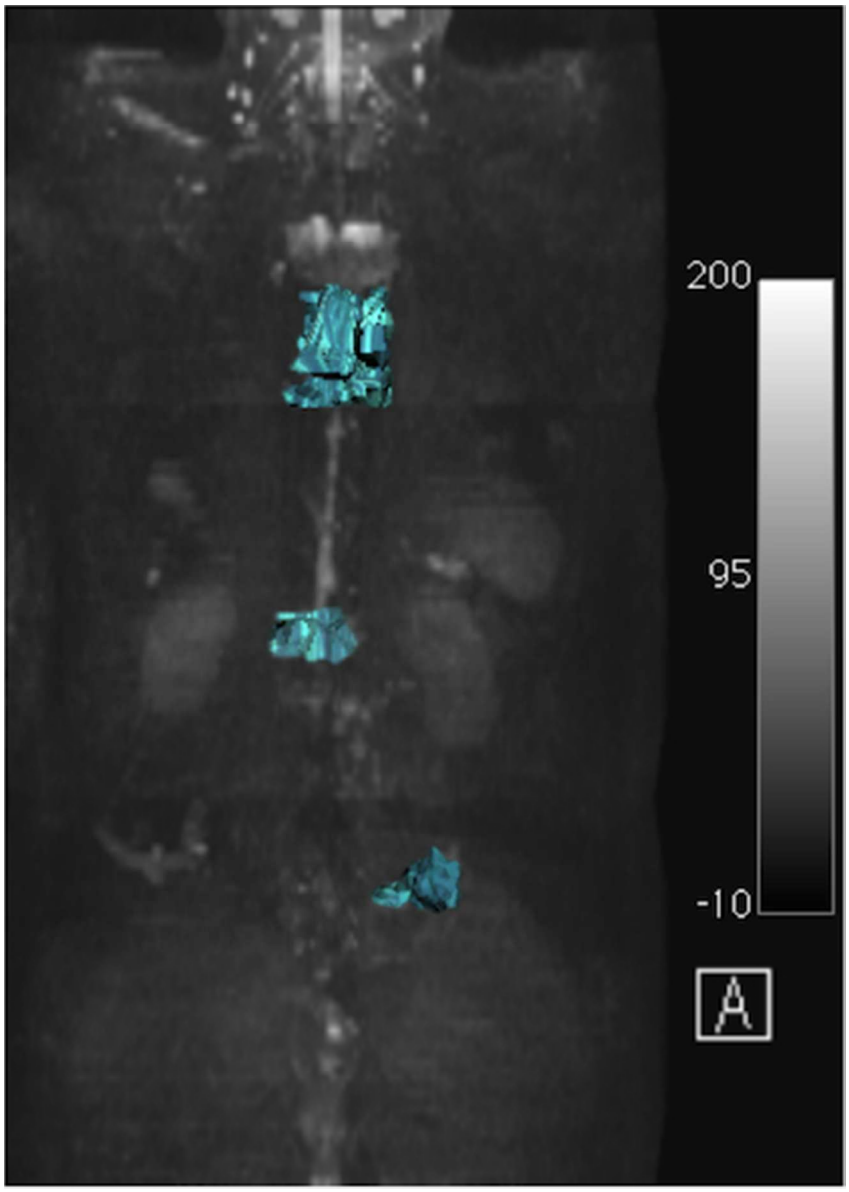

Figure 3b. Images of mCRPC in a 70-year-old man responding to olaparib showing reduction in the b900 DWI signal abnormality extent on maximum intensity projection images (b=900 s/mm^2) at baseline (a) and after 12 weeks of treatment (b). The histogram (c) depicts the ADC values of the tDV at baseline and after 12 weeks on treatment, showing an increase in the mADC.

Figure 3
35x50mm (300 x 300 DPI)

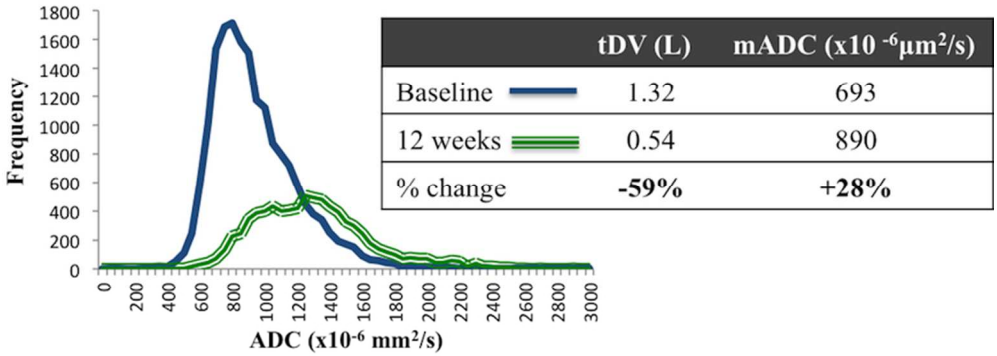

Figure 3c. Images of mCRPC in a 70-year-old man responding to olaparib showing reduction in the b900 DWI signal abnormality extent on maximum intensity projection images (b=900 s/mm^2) at baseline (a) and after 12 weeks of treatment (b). The histogram (c) depicts the ADC values of the tDV at baseline and after 12 weeks on treatment, showing an increase in the mADC.

73x29mm (300 x 300 DPI)

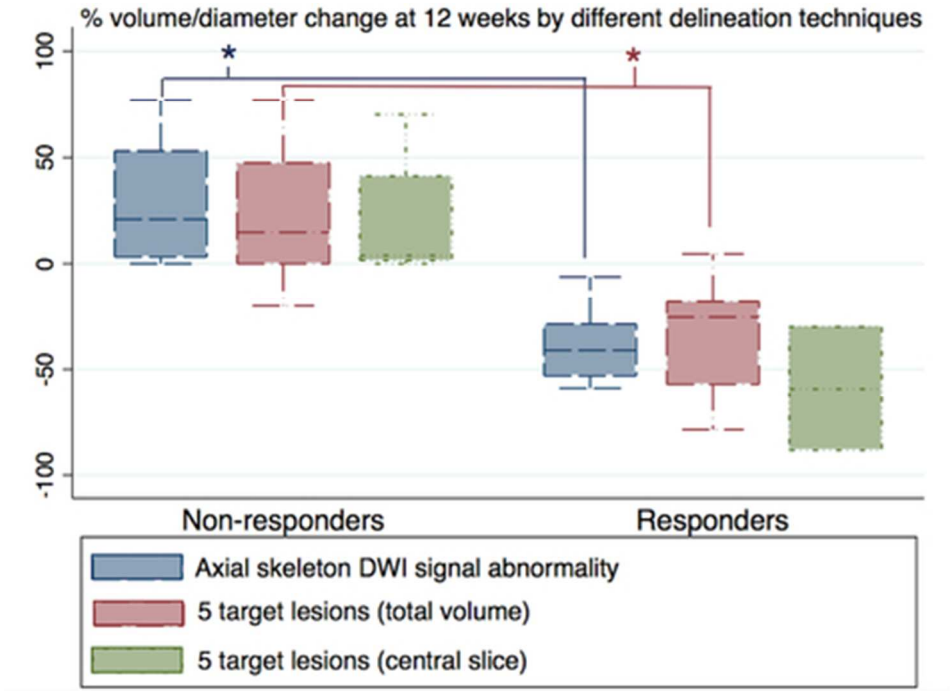

Appendix figure 1a. Box-plots of (a) percentage volume/diameter change of bone metastases, delineated on axial DWb900, and (b) median apparent diffusion coefficient (mADC) at 12 weeks assessed by different delineation techniques.
* Logistic regression ($p<0.05$)

Appendix figure 1
39x29mm (300 x 300 DPI)

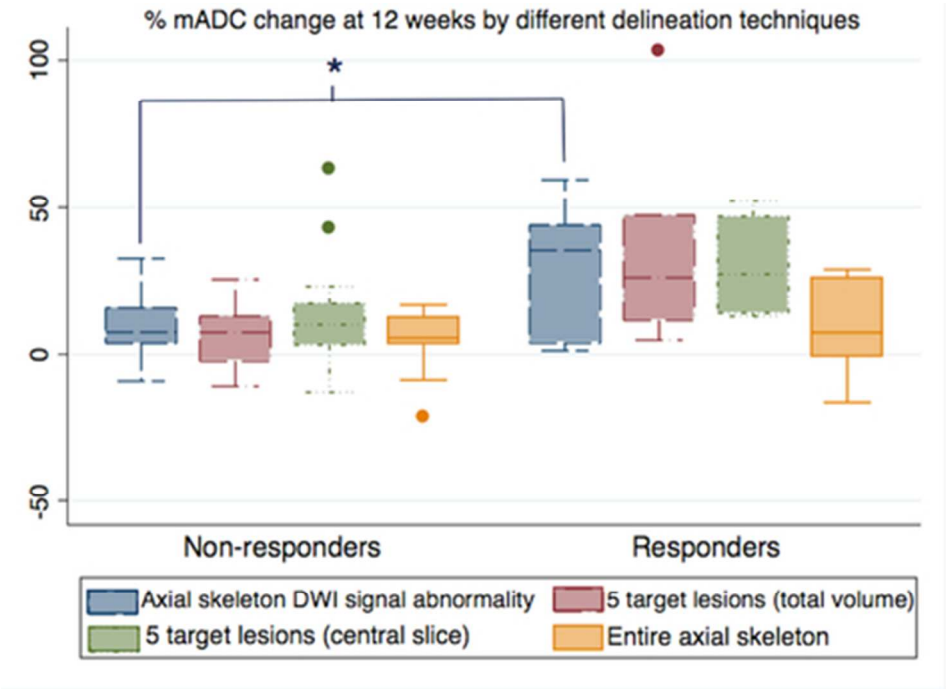

Appendix figure 1b. Box-plots of (a) percentage volume/diameter change of bone metastases, delineated on axial DWb900, and (b) median apparent diffusion coefficient (mADC) at 12 weeks assessed by different delineation techniques.
* Logistic regression ($p<0.05$)

Appendix figure 1
39x29mm (300 x 300 DPI)

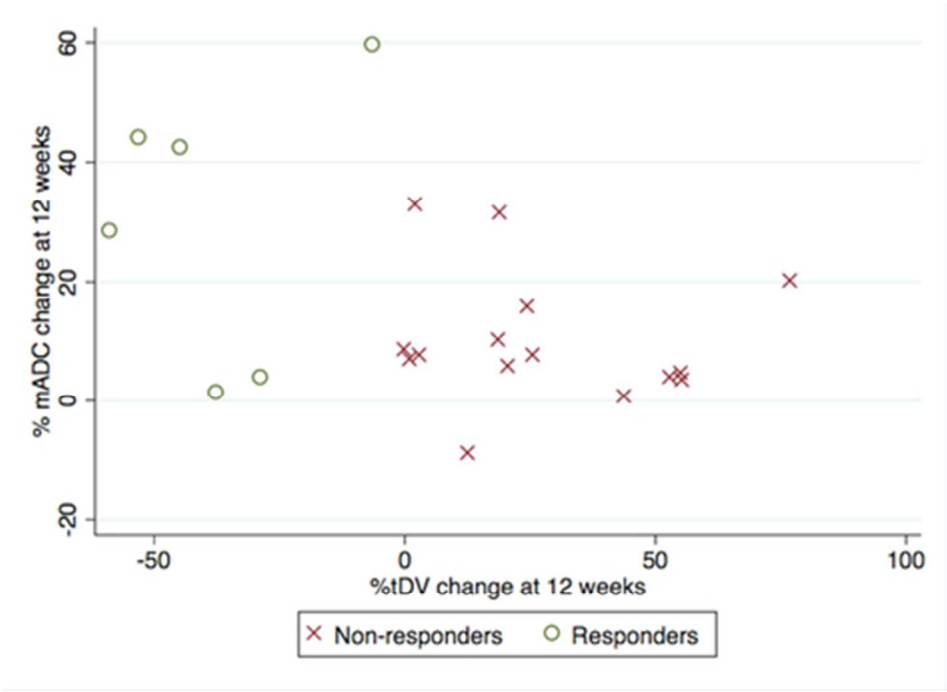

Appendix figure 2. Scatter plot of total diffusion volume (tDV) and median apparent diffusion coefficient (mADC) change when delineating axial skeleton diffusion signal abnormality in responders (green circles) and non-responders (red crosses).
Appendix figure 2
39x29mm (300 x 300 DPI)

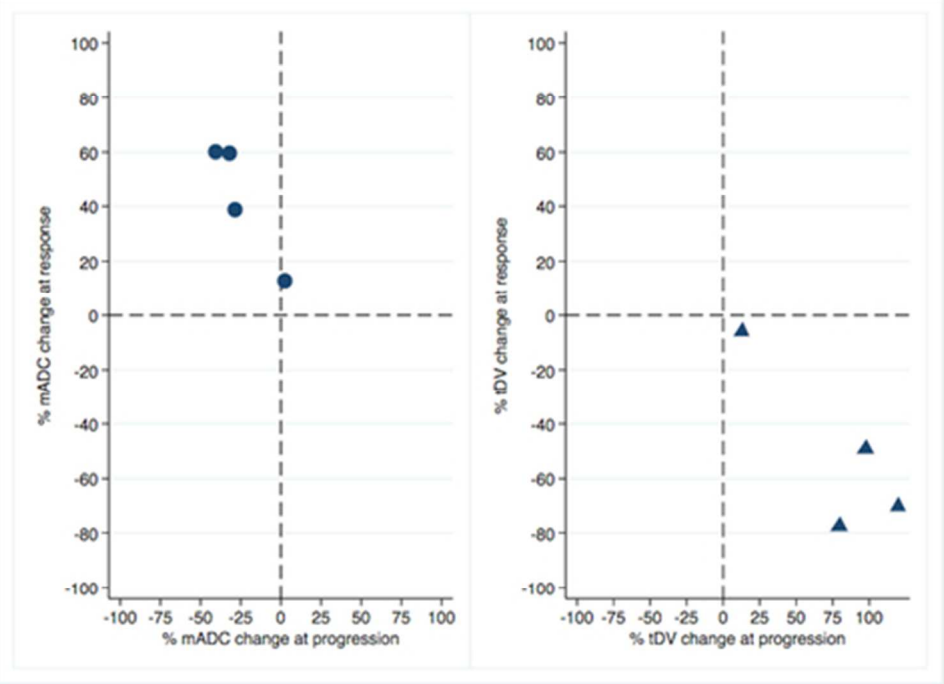

Appendix figure 3. Scatter plots of percentage change of total diffusion volume (tDV) (triangles) and median apparent diffusion coefficient (mADC) (circles) at response and disease progression in those 4 responder patients with evaluable whole body MRI.
Appendix figure 3
39x29mm (300 x 300 DPI)

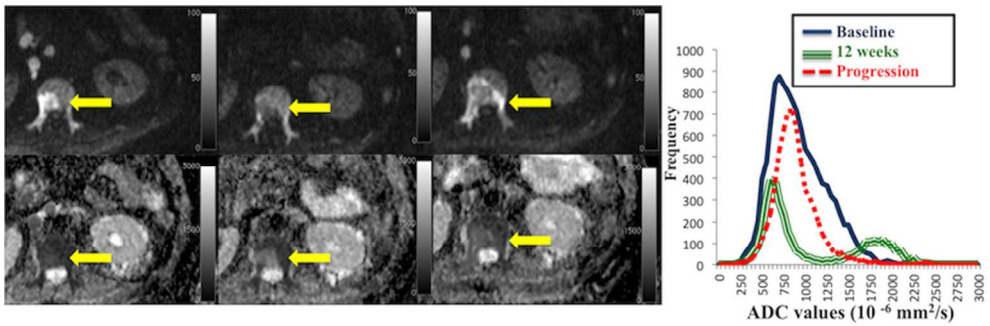

Appendix figure 4. Images in a 70-year-old mCRPC man on olaparib. Initially, the 12 weeks axial MRI images showed a reduction of the DWI (b = 900 mm/s^2) signal abnormality extent in the lumbar vertebrae bone metastases and an increase in mADC values compared to baseline; subsequently a follow-up MRI showed an increase of signal abnormality extent on DWI (b = 900 mm/s^2) and a decrease in the mADC values in the same bone metastases, in keeping with disease progression. The histogram depicts the ADC values of the tDV at baseline, after 12 weeks on treatment and at progression.
Appendix figure 4
92x29mm (300 x 300 DPI)

STROBE Statement—checklist of items that should be included in reports of observational studies

	Item No	Recommendation	✔ (N/A)
Title and abstract			
	1	(*a*) Indicate the study's design with a commonly used term in the title or the abstract	✔ page 5 line 21
		(*b*) Provide in the abstract an informative and balanced summary of what was done and what was found	✔ page 5 lines 27-60
Introduction			
Background/rationale	2	Explain the scientific background and rationale for the investigation being reported	✔ page 7 lines 22-44
Objectives	3	State specific objectives, including any prespecified hypotheses	✔ page 8 lines 6-26
Methods			
Study design	4	Present key elements of study design early in the paper	✔ page 9 lines 6-46
Setting	5	Describe the setting, locations, and relevant dates, including periods of recruitment, exposure, follow-up, and data collection	✔ page 8 lines 38-48
Participants	6	(*a*) *Cohort study*—Give the eligibility criteria, and the sources and methods of selection of participants. Describe methods of follow-up *Case-control study*—Give the eligibility criteria, and the sources and methods of case ascertainment and control selection. Give the rationale for the choice of cases and controls *Cross-sectional study*—Give the eligibility criteria, and the sources and methods of selection of participants	✔ page 9 line 51 to page 10 line 14
		(*b*) *Cohort study*—For matched studies, give matching criteria and number of exposed and unexposed *Case-control study*—For matched studies, give matching criteria and the number of controls per case	N/A
Variables	7	Clearly define all outcomes, exposures, predictors, potential confounders, and effect modifiers. Give diagnostic criteria, if applicable	✔ page 9 lines 36-46
Data sources/ measurement	8*	For each variable of interest, give sources of data and details of methods of assessment (measurement). Describe comparability of assessment methods if there is more than one group	✔ page 10 line 52 to page 12 line 12
Bias	9	Describe any efforts to address potential sources of bias	✔ page 12 lines 30-34
Study size	10	Explain how the study size was arrived at	✔ page 9 line

			51 to page 10 line 14
Quantitative variables	11	Explain how quantitative variables were handled in the analyses. If applicable, describe which groupings were chosen and why	✔ page 12 lines 20-30
Statistical methods	12	(*a*) Describe all statistical methods, including those used to control for confounding	✔ page 12 lines 20-50
		(*b*) Describe any methods used to examine subgroups and interactions	N/A
		(*c*) Explain how missing data were addressed	N/A
		(*d*) *Cohort study*—If applicable, explain how loss to follow-up was addressed *Case-control study*—If applicable, explain how matching of cases and controls was addressed *Cross-sectional study*—If applicable, describe analytical methods taking account of sampling strategy	N/A
		(*e*) Describe any sensitivity analyses	N/A

Prudential Tower, 800 Boylston Street, 15th Floor, Boston, MA 02199

Results			✔ (N/A)
Participants	13*	(a) Report numbers of individuals at each stage of study—eg numbers potentially eligible, examined for eligibility, confirmed eligible, included in the study, completing follow-up, and analysed	✔ page 9 line 51 to page 10 line 14
		(b) Give reasons for non-participation at each stage	✔ page 9 line 51 to page 10 line 14
		(c) Consider use of a flow diagram	✔ page 13 line 26
Descriptive data	14*	(a) Give characteristics of study participants (eg demographic, clinical, social) and information on exposures and potential confounders	✔ page 13 line 6-28
		(b) Indicate number of participants with missing data for each variable of interest	✔ page 13 line 14-22
		(c) *Cohort study*—Summarise follow-up time (eg, average and total amount)	✔ page 9 line 30-36
Outcome data	15*	*Cohort study*—Report numbers of outcome events or summary measures over time	✔ page 9 line 51 to page 10 line 14
		Case-control study—Report numbers in each exposure category, or summary measures of exposure	N/A
		Cross-sectional study—Report numbers of outcome events or summary measures	N/A
Main results	16	(*a*) Give unadjusted estimates and, if applicable, confounder-adjusted estimates and their precision (eg, 95% confidence interval). Make clear which confounders were adjusted for and why they were included	✔ page 12 line 30-48
		(*b*) Report category boundaries when continuous variables were categorized	N/A
		(*c*) If relevant, consider translating estimates of relative risk into absolute risk for a meaningful time period	N/A
Other analyses	17	Report other analyses done—eg analyses of subgroups and interactions, and sensitivity analyses	✔ page 9 line 30-34
Discussion			
Key results	18	Summarise key results with reference to study objectives	✔ page 17 line 48 to page 18 line 32

Limitations	19	Discuss limitations of the study, taking into account sources of potential bias or imprecision. Discuss both direction and magnitude of any potential bias	✔ page 19 line 12-40
Interpretation	20	Give a cautious overall interpretation of results considering objectives, limitations, multiplicity of analyses, results from similar studies, and other relevant evidence	✔ page 19 line 40-50
Generalisability	21	Discuss the generalisability (external validity) of the study results	✔ page 20 line 6-18
Other information			
Funding	22	Give the source of funding and the role of the funders for the present study and, if applicable, for the original study on which the present article is based	✔ page 9 line 18-24 and page 21 line 7-39

*Give information separately for cases and controls in case-control studies and, if applicable, for exposed and unexposed groups in cohort and cross-sectional studies.

Note: An Explanation and Elaboration article discusses each checklist item and gives methodological background and published examples of transparent reporting. The STROBE checklist is best used in conjunction with this article (freely available on the Web sites of PLoS Medicine at http://www.plosmedicine.org/, Annals of Internal Medicine at http://www.annals.org/, and Epidemiology at http://www.epidem.com/). Information on the STROBE Initiative is available at www.strobe-statement.org.

*N/A stands for not applicable and may be a reasonable choice depending on the type of study performed